Towards a self consistent evaluation of the RF wave-field and the ion distribution functions in tokamak plasmas

N. Bertelli[1], E. Valeo[1], J. P. Lee[2], P. Bonoli[2], M. Gorelenkova[1], D. L. Green[3], E. F. Jaeger[4], C. K. Phillips[1] and J. C. Wright[2]

[1]Princeton Plasma Physics Laboratory, Princeton, NJ 08543, USA
[2]Plasma Science and Fusion Center, MIT, Cambridge, MA 02139, USA
[3]Oak Ridge National Laboratory, PO Box 2008, Oak Ridge, TN 37831-6169, USA
[4]XCEL Engineering Inc., 1066 Commerce Park Drive, Oak Ridge, TN 37830, USA

Corresponding Author: nbertell@pppl.gov

Abstract:
The injection of fast waves (FW) in the ion cyclotron range of frequency (ICRF) is a well-established method of heating and driving current in magnetically confined toroidal plasma and it will play an important role in the ITER experiment. Taking into account self-consistently the interaction of FW with both the minority ion population and fast-ion / neutral beam populations is a crucial aspect to more faithfully model and understand experimental results and to more accurately design future devices. This paper examines precisely this aspect combining the evaluation of the wave-field, through a full wave solver, with the ion distribution function provided by either an analytical functional form or a Monte-Carlo particle code. The recent extension of TORIC v.5 to include non-Maxwellian distribution functions (both in minority and high harmonic heating regimes) is employed in this work. First, for the case of the thermal distribution function, the extended TORIC v.5 has been verified against the standard TORIC v.5 showing an excellent agreement both in IC minority and high harmonic fast wave (HHFW) heating regimes. Second, an implementation of the bi-Maxwellian and analytical distributions has also been done. The application of such distributions shows different behavior in the total absorbed power between the IC minority and HHFW heating regimes. Third, a comparison of the total power deposition profile with a Maxwellian and a numerical distribution function obtained from the Monte-Carlo NUBEAM module is presented.

1 Introduction

Fast wave (FW) heating in the ion cyclotron range of frequency (ICRF) has been successfully used to sustain and control the fusion plasma performance, and it will likely play an important role in the ITER experiment. As demonstrated in the NSTX and DIII-D experiments the interactions between fast waves and fast ions can be so strong to significantly modify the fast ion population from neutral beam injection (NBI). In fact, it has been found in NSTX that FWs can modify and, under certain conditions, even suppress the energetic particle driven instabilities, such as toroidal Alfvén eigenmodes (TAEs) and global Alfvén eigenmodes (GAEs) and fishbones [1, 2, 3]. Similarly, the non-Maxwellian effects play an important role in the interaction between FWs and ion minority species in the IC minority heating scheme. In particular, the distribution function modifications will, generally, result in finite changes in the amount and spatial location of absorption. All these aspects will also play a major role in ITER and they are examined in this paper combining the evaluation of the wave-field, through a full wave solver, with the ion distribution function provided by either an analytical functional form or a Monte-Carlo particle codes. More specifically, in this paper we employ the recent extension of TORIC v.5 to include non-Maxwellian distribution functions both in minority and high harmonic heating regimes. Similar progress has been done in our community with different RF numerical tools [4, 5, 6, 7, 8, 9] and references within. This paper is structured as follows: in section 2, a brief description of the extension code and parameters used in the simulation are summarized. In section 3 a test for a Maxwellian case is presented for Alcator C-Mod and NSTX plasmas. Results for a bi-Maxwellian distribution and a numerical particles list from NUBEAM Monte-Carlo code for a NSTX tokamak plasma are shown in Section 4 and 5, respectively. Finally, a brief discussion is presented in section 6.

2 TORIC extension and parameters adopted

In the original version of TORIC code [10, 11, 12], the elements of the local susceptibility tensor, $\chi_i j$, are restricted to the Maxwellian case. In order to take into account the non-Maxwellian effects, the recent TORIC extension [13] includes a generalization of the components of χ in the minority and high harmonic fast wave (HHFW) heating regimes. More specifically,

- in the minority heating regimes, the components of χ are implemented up to the second order in $k_\perp v_\perp/\omega_c$ (where $k_\perp$, $v_\perp$, ands ω_c are the perpendicular component of the wave-vector, the perpendicular component of the particle velocity, and the ion cyclotron angular frequency, respectively) and for arbitrary velocity distribution functions [14];

- in HHFW heating regime, the components of χ correspond to the full-hot susceptibility tensor for arbitrary velocity distribution functions without any restriction in the finite Larmor radius (FLR) order and in the harmonic numbers (see Eq. 48 in page 255 of Stix's book [15]).

The version of TORIC employed in this work is, so-called, version 5, which is currently implemented in the TRANSP code [16].

Simulations are shown in minority and HHFW heating regimes for Alcator C-Mod [17] and NSTX [18] plasmas, respectively. The toroidal field at the magnetic axis is 5 (0.53) Tesla for Alcator C-Mod (NSTX) case. The magnetic axis major radius is 68.26 (101.34) cm for Alcator C-Mod (NSTX) case. The core ($\rho = 0$) electron density and the core electron and ion temperatures are 1.78×10^{14} cm^{-3}, $T_e = 2.8$ keV, and $T_i = 2.2$ keV for Alcator C-Mod case, respectively. The core electron density and the core electron and ion temperatures are 2.47×10^{13} cm^{-3}, $T_e = 1.1$ keV, and $T_i = 1.1$ keV for NSTX case, respectively. The equivalent core temperature for the fast ions generated by NBI is about 21 keV. For Alcator C-Mod case: the plasma consists of 7% fractional number density of hydrogen and 93% deuterium. The wave parameters are: frequency $f = 78$ MHz and toroidal wavenumber $n_\phi = 10$, which places the fundamental H and second harmonic D resonances at .62 cm radially with respect to the magnetic axis location. For NSTX case: the plasma consists of about 86.5% fractional number of density of (thermal) deuterium and 8% of beam deuterium (fast ions). The wave parameters are: frequency $f = 30$ MHz and toroidal wavenumber $n_\phi = 8$, which places the second and eleventh harmonic D resonances at the very edge of the high-field side and the low-field side, respectively.

3 Maxwellian test

In order to test the implementation and the algorithm of the code extension, we first compare the reference calculation obtained from the original version of the code which assumes an isotropic Maxwellian distributions (using the plasma Z function to evaluate χ) with the susceptibility calculated numerically as described in Section 2 for a Maxwellian distribution prescribed on a uniform numerical mesh.

Figure 1 shows the two cases considered here: figure 1(a) is the contour plot of the right-handed wave electric field, Re(E_-), where $E_- = E_x - iE_y$ (in Stix coordinates) for an Alcator C-Mod plasma while figure 1(b) is the contour plot of the Re(E_-), for a NSTX plasma.

- For minority heating regime: the relative power absorbed by second harmonic D, fundamental H and by the electrons for each wave branch is presented in Table I(left) in the column labeled "Reference". To check the accuracy of the method, the results were re-computed with the minority H susceptibility calculated numerically for a Maxwellian distribution prescribed on a uniform numerical mesh of $N_{v_\parallel} = 500$ points and $N_{v_\perp} = 100$ points. The mesh range is $-c/100 \leqslant v_\parallel \leqslant c/100$, $0 \leqslant v_\perp \leqslant c/100$ where $c = 3 \times 10^{10}$ cm/s is the speed of light. As shown in Table I(left) an excellent agreement is found with differences is less than $1 - 2\%$.

- For HHWF heating regime: the relative power absorbed by thermal D, fast ions (D-NBI) and by the electrons is presented in Table I(right) in the column labeled "Reference". Again, to check the accuracy of the method, the results were re-computed with the fast ions (D-NBI) susceptibility calculated numerically for a Maxwellian distribution prescribed on a uniform numerical mesh of $N_{v_\parallel} = 100$ points and $N_{v_\perp} = 50$ points. The mesh range is $-c/20 \leqslant v_\parallel \leqslant c/20$, $0 \leqslant v_\perp \leqslant c/20$. As shown in Table I(right) an excellent agreement is found with differences is less than 1%.

For both heating regimes, other cases with different resolutions (not shown here) have been performed always obtaining an excellent agreement between reference and numerical cases in terms of electric field propagation, power density profiles, and total absorbed power.

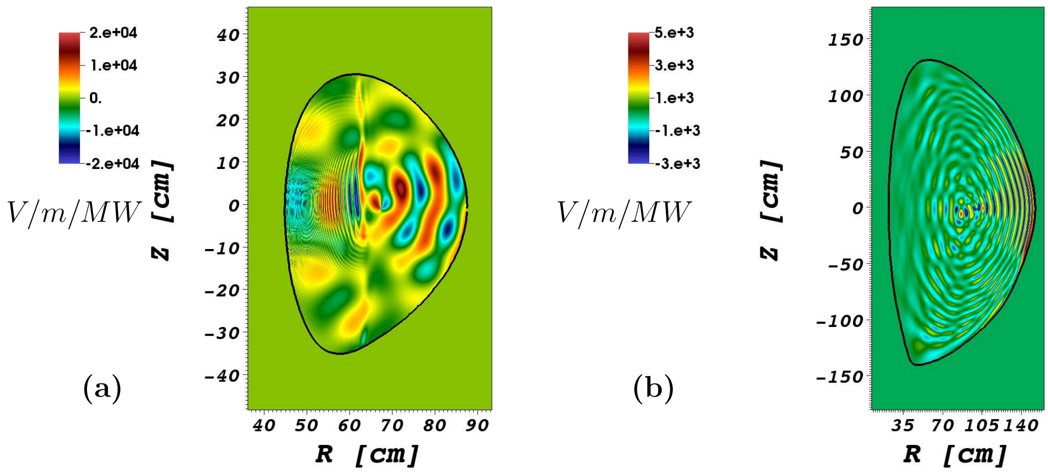

FIG. 1: Real part of the right-handed wave electric field, Re(E_-), for an Alcator C-Mod (figure (a)) and NSTX (figure (b)) plasmas described in section 2.

Abs. fraction	Reference	Numerical	Abs. fraction	Reference	Numerical
2nd Harmonic D	10.18	10.28	D	0.22	0.22
Fundamental H	69.95	68.81	D - NBI	73.88	73.58
Electrons - FW	11.35	11.91	Electrons	25.90	26.21
Electrons - IBW	8.53	9.00			

TABLE I: Power flow to each species for Alcator C-Mod case (left table) and NSTX case (right table). "Reference" corresponds to the original Maxwellian case while "Numerical" numerically computed minority H susceptibility assuming a Maxwellian distribution function.

4 Bi-Maxwellian distribution function

In this section we present the first application of the TORIC extension assuming a bi-Maxwellian distribution function for H and fast ions (D-NBI) susceptibilities for Alcator C-Mod and NSTX cases, respectively. In particular, the distribution functions has the following form

$$f_{\mathrm{H,D}}(v_\parallel, v_\perp) = (2\pi)^{-3/2}(v_{\mathrm{th},\parallel} v_{\mathrm{th},\perp}^2)^{-1} \exp[-(v_\parallel/v_{\mathrm{th},\parallel})^2 - (v_\perp/v_{\mathrm{th},\perp})^2] \qquad (1)$$

with $v_{\mathrm{th},\parallel} = \sqrt{2C_\parallel T(\psi)/m_{\mathrm{H,D}}}$ and $v_{\mathrm{th},\perp} = \sqrt{2C_\perp T(\psi)/m_{\mathrm{H,D}}}$. Two constants $C_\parallel$ and $C_\perp$ have been introduced to perform a scan in both parallel and perpendicular temperatures computing the sensitivity of the H and fast ions absorption for Alcator C-Mod and NSTX cases, respectively.

- For minority heating regime: the fundamental H absorption fraction, P_{H}, varied by less than two percent when $C_\perp$ was varied from .5 to 5, with $C_\parallel$ held fixed at unity. In contrast the second series, in which $C_\perp$ was fixed at unity and $C_\parallel$ was varied shows a significant variation. For $C_\parallel = \{.5, 1., 3., 5.\}$, the corresponding $P_{\mathrm{H}} = \{61.27, 70.50, 90.46, 94.18\}$. In addition, while the absorption profile is localized to the resonant layer for small $C_\parallel$ it is significantly broadened radially at for large $C_\parallel$. This is clearly demonstrated in Figure 2 where the absorption vs. (R,Z) is shown for $C_\parallel = .5$ (Fig. 2(a)), $C_\parallel = 1.0$ (Fig. 2(b)), and $C_\parallel = 5.$ (Fig. 2(c)).

- For HHWF heating regime: the fast ions absorption fraction, $P_{\mathrm{D-NBI}}$, shows a significant variation when $C_\perp$ was varied from .5 to 5, with $C_\parallel$ held fixed at unity. In particular, for $C_\perp = \{.5, 1., 3., 5.\}$, the corresponding $P_{\mathrm{D-NBI}} = \{70.06; 73.56; 62.84; 48.48\}$. In contrast, when $C_\perp$ was fixed at unity and $C_\parallel$ was varied showed, $P_{\mathrm{D-NBI}}$, varied by less than one percent. However, the absorption profile tends to be localized to the resonant layer for small $C_\parallel$ as shown in Figure 3. In this figure the absorption vs. (R,Z) is shown for $C_\parallel = .5$ (Fig. 3(a)), $C_\parallel = 1.0$ (Fig. 3(b)), and $C_\parallel = 5.$ (Fig. 3(c)). Similar results are found when a slowing down distribution function was employed (not show here).

5 NUBEAM particle list

In this section we show an applicaton of the TORIC extension by using a numerical distribution function. More specifically, we use the P2F code [19] to generate a continuum distribution function starting from a particles list from the NUBEAM Monte-Carlo particles code [20, 21].

Since the full-wave code, such as TORIC code, takes velocity space derivatives of the beam distribution function to obtain the components of the susceptibility tensor that function must be smooth enough for the derivatives to be robust. In order to achieve this, we employ the P2F code, which converts an input discrete particle list to a 4-D continuum distribution function. The four dimensions are two cylindrical in space (R, z) and two cylindrical in velocity space $(v_\perp, v_\parallel)$ with parallel being along the local B field direction. A distribution function obtained by P2F is shown in Figure 4 using a NUBEAM particle list with 53115 number of particles for NSTX discharge 141711 (at $t = 0.470$ s) on the magnetic axis. One can see that the maximum particles energy is 90 keV (white curve in the figure), which corresponds to the injected energy of the beam ions. As similarly done above, a comparison between the equivalent Maxwellian case (namely, the beam ions temperature is $T_{\mathrm{bi}} = \frac{2}{3}\frac{E}{n_{\mathrm{fast}}}$, where E and n_{fast} are the total energy density profile and the density of the beams ions, respectively) and the numerical calculation (real distribution:

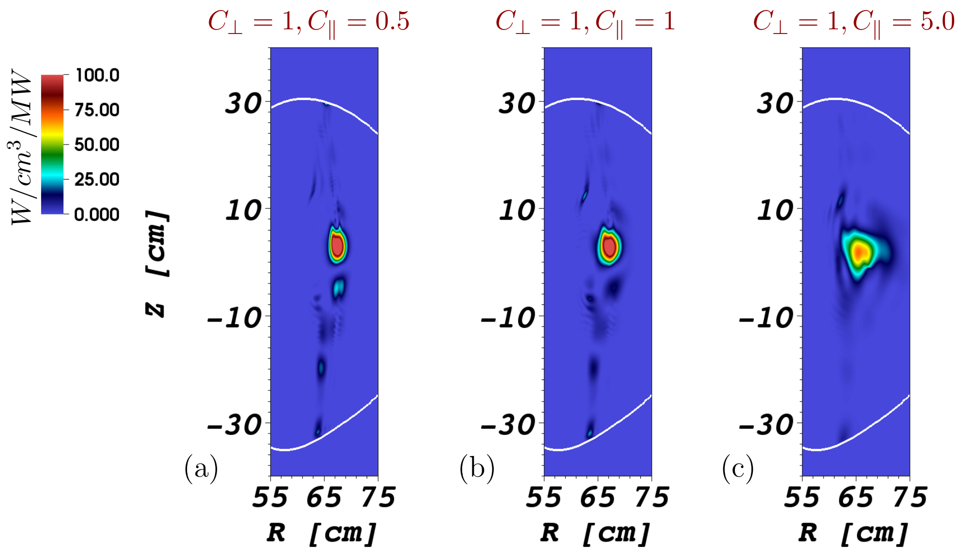

FIG. 2: Contour plots of fundamental absorption by minority hydrogen (zoomed around the resonance), represented by a bi-Maxwellian distribution function (see Eq. 1) in an Alcator C-Mod plasma for $C_\perp = 1.0$ and different $C_\parallel$ values (shown in the plots). The white curve represents the last closed flux surface. Units are Watts/cm^3 at 1MW incident power.

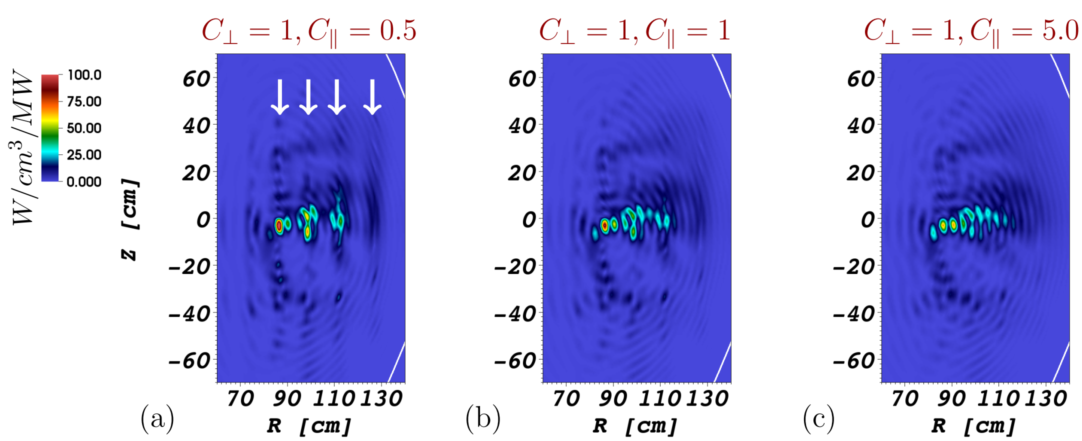

FIG. 3: Contour plots of the absorption by beam ions (zoomed around the cyclotron resonances) represented by a bi-Maxwellian distribution function in a NSTX plasma for $C_\perp = 1.0$ and different $C_\parallel$ values (shown in the plots). The white curve represents the last closed flux surface. The white arrows in figure (a) indicates the deuterium cyclotron resonance layers ($n = 7, 8, 9,$ and 10). Units are Watts/cm^3 at 1MW incident power.

non-Maxwellian case) has been performed. In table 4(b), we show the differences in the power flows to each species between the Maxwellian and non-Maxwellian case. As expected, a slightly larger amount of power flows to fast ions when taking into account a realistic distribution function. This is due to the fact that a larger number of particles with larger energy interact with fast waves on the cyclotron resonances in the plasma.

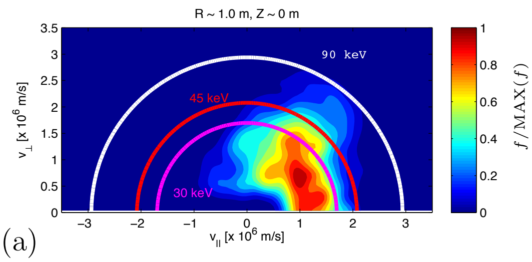

(a)

Abs. fraction	f Maxw.	f non-Maxw.
Electrons	41.80 %	37.99 %
D-NBI	53.94 %	58.12 %

(b)

FIG. 4: (a) Distribution function obtained from P2F code starting from a NUBEAM particles list for a NSTX plasma without HHFW. (b) Power flow to each species for and NSTX case. "f Maxw." corresponds to the equivalent Maxwellian case while "f non-Maxw." numerically computed by using the realistic distribution function from NUBEAM shown figure (a)).

6 Conclusions and discussion

In summary, the first applications of the recent TORIC extension to include non-Maxwellian ion effects have been presented for minority and HHFW heating regimes. The application of bi-Maxwellian distribution function shows a different behavior in the total absorbed power between the most common IC minority and HHFW heating regimes. In particular, for IC minority heating regime, the total absorbed power at the H fundamental is insensitive to variations in the perpendicular temperature ($T_\perp$), but varies with changes in parallel temperature ($T_\parallel$), whereas for HHFW regime, the behavior is the other way around, namely, the total absorbed power by fast ions is insensitive to variations in $T_\parallel$. However, for both heating regimes, the power density profiles vary with changes in $T_\parallel$. Finally, a realistic distribution function obtained from a NUBEAM particle list for a NSTX plasma has been used. The result indicates a slightly larger amount of power flows to fast ions when non-Maxwellian effects are considered. This is a first step towards closing the loop between the extension of TORIC in a self-consistent way and the NUBEAM code (which includes a RF kick heating operator) for a NSTX-U plasma. In this scenario, we might expect a larger amount of power deposited to the fast ions population due to a larger distribution function tail formed by the RF application. Additionally, the quasilinear diffusion coefficients for the finite Larmor radius (FLR) approximation (valid for the IC minority regimes) have been derived and implemented in TORIC v.5 [22]. A self-consistent distribution function will be then obtained by iterating between TORIC and the Fokker-Planck code CQL3D [23, 24], which are coupled through the quasilinear diffusion coefficients and the non-Maxwellian dielectric tensor.

7 Acknowledgments

This work was supported by the SciDAC Center for Wave-Plasma Interactions under DE-FC02-01ER54648 and the US DOE under DE-AC02-CH0911466.

References

[1] FREDRICKSON, E.D., et al., Nucl. Fusion **55**, 013012 (2015).

[2] PODESTÀ,M., et al., Nucl. Fusion **52**, 094001 (2012).

[3] HEIDBRINK, W. W., et al., Plasma Phys. Control. Fusion **48**, 1347 (2006).

[4] JAEGER, E. F., et al., Phys. Plasmas **13**, 056101 (2006).

[5] MURAKAMI, S., et al., Nucl. Fusion **46**, S425 (2006).

[6] BRAMBILLA, M. and BILATO, R., Nucl. Fusion **49**, 085004 (2009).

[7] BILATO, R., et al., Nucl. Fusion **51**, 103034 (2011).

[8] CHOI, M., et al., pop **17**, 056102 (2010).

[9] JUCKER, M., et al., Comp. Phys. Comm. **182**, 912 (2011).

[10] BRAMBILLA, M., Plasma Phys.Controlled Fusion **41**, 1 (1999).

[11] BRAMBILLA, M., Plasma Phys.Controlled Fusion **44**, 2423 (2002).

[12] WRIGHT, J. C., et al., Nucl. Fusion **45**, 1411 (2005).

[13] BERTELLI, N., et al., paper in preparation

[14] PHILLIPS, C. K., et al., AIP Conference Proceedings **694**, 499 (2003).

[15] STIX,T. H. , Waves in Plasmas (American Institute of Physics, NY, 1992).

[16] HAWRYLUK, R. J., 1980 Physics Close to Thermonuclear Conditions vol 1 ed B. Coppi et al (Brussels: Commission of the European Communities) p 19.

[17] BONOLI, P. T., et al., Fusion Science and Technology **51**, (2007) 401.

[18] KAYE, S. M., et al., Nucl. Fusion **55** (2015) 104002.

[19] GREEN, D. L. Green, et al., Journal of Physics: Conference Series **180**, 012058 (2009);

[20] GOLDSTON, R.J., et al., J. Comput. Phys. **43**, 61 (1981).

[21] PANKIN, A., et al., Comput. Phys. Commun. **159**, 157 (2004).

[22] LEE, J. P., et al., Bull Am. Phys. Soc **60**, 242 (2015) (`http://meetings.aps.org/link/BAPS.2015.DPP.NP12.51`)

[23] HARVEY, R. W., and MCCOY,M.G., Proc. IAEA TCM on Advances in Sim. and Modeling of Thermonuclear Plasmas, pp. 489-526, Montreal, (1992).

[24] PETROV, Yu. V. and HARVEY, R. W., Plasma Phys. Control. Fusion **58**, 115001 (2016).